Journal of Aircraft

VOLUME 6 NOVEMBER-DECEMBER 1969 NUMBER 6

Energy-State Approximation in Performance Optimization of Supersonic Aircraft

ARTHUR E. BRYSON JR.* AND MUKUND N. DESAI†
Harvard University, Cambridge, Mass.

AND

WILLIAM C. HOFFMAN‡
Kaman AviDyne, Burlington, Mass.

The use of the energy-state approximation for airplane performance optimization is extended to maximum-range problems. Until now it has been applied only to minimum-time and minimum-fuel climb problems. Numerical performance results for typical supersonic aircraft are presented for both range and climb problems. These compare favorably with the results obtained using more complicated dynamic models.

Nomenclature

C_D = drag coefficient
C_{D_0} = drag coefficient at zero lift
C_L = lift coefficient
C_{L_α} = lift coefficient slope, rad^{-1}
D = drag, lb
E = energy per unit mass, ft^2/sec^2
H = variational Hamiltonian
L = lift, lb
M = Mach number (V/a)
R = range traversed, ft
S = aerodynamic reference area, ft^2
T = thrust, lb
V = velocity, fps
a = speed of sound, fps
c = specific impulse of powerplant, sec
f = fuel flow rate, slug/sec
g = acceleration of gravity, 32.2 ft/sec^2
h = altitude, ft
m = mass, slugs
q = dynamic pressure, lb/ft^2
t = time, sec
x = horizontal distance, ft
α = angle of attack, rad
γ = flight-path angle, rad
ϵ = angle between thrust axis and zero-lift axis, rad
η = induced drag parameter, rad^{-1}
λ = influence function
μ = fuel mass expended, slugs
ρ = atmospheric density, lb-sec^2/ft^4
ϕ = maximum range for an unpowered glide, ft

Subscripts

f = final value
max = maximum value
min = minimum value
0 = initial value
s = stalling speed value
1 = intermediate value

Superscripts

$(\bar{\ })$ = average value
$(\dot{\ })$ = time derivative

Introduction

THE amount of difficulty and expense experienced in calculating optimal flight paths depends primarily upon the complexity of the dynamic model used to describe the aircraft. The models used range from a simple point-mass quasi-steady representation to models that include deflections of the airframe. For performance prediction, a point-mass model for motion in a vertical plane is usually quite adequate. Figure 1 shows the nomenclature commonly used for this model.

The equations of motion for this model are

$$m\dot{V} = T\cos(\alpha + \epsilon) - D - mg\sin\gamma \quad (1)$$

$$mV\dot{\gamma} = T\sin(\alpha + \epsilon) + L - mg\cos\gamma \quad (2)$$

$$\dot{h} = V\sin\gamma \quad (3)$$

$$\dot{x} = V\cos\gamma \quad (4)$$

Presented as Paper 68-877 at the AIAA Guidance, Control, and Flight Dynamics Conference, Pasadena, Calif., August 12-14, 1968; submitted January 3, 1969; revision received May 9, 1969. This research was supported in part by NASA Grant NGR-22-007-068 and ONR Contract Nonr-1866(16).

* Professor, Division of Engineering and Applied Physics; now Professor, Applied Mechanics Department, Stanford University, Stanford, Calif. Fellow AIAA.
† Research Assistant.
‡ Staff Scientist. Associate Member AIAA.

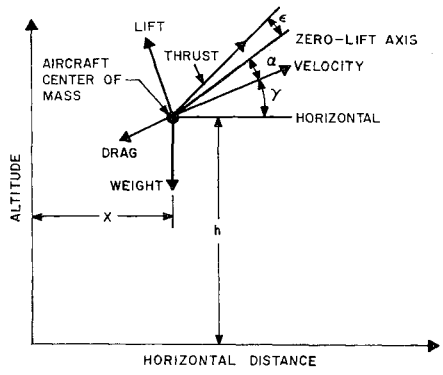

Fig. 1 Nomenclature used in analysis of supersonic interceptors.

$$\dot{m} = -f \tag{5}$$

where the state variables are velocity V, flight-path angle γ, altitude h, horizontal range x, and mass m, and where $T = T(V,h)$ = thrust, $D = D(V,h,\alpha)$ = drag, $L = L(V,h,\alpha)$ = lift, α = angle of attack (measured from zero-lift axis), g = acceleration of gravity, $f = f(V,h)$ = fuel flow rate, and ϵ = angle between thrust axis and zero-lift axis, assumed given. Since both α and ϵ are small, Eqs. (1) and (2) can be simplified by using the small angle approximation

$$\sin(\alpha + \epsilon) \cong \alpha + \epsilon, \cos(\alpha + \epsilon) \cong 1 \tag{6}$$

This paper is concerned with further approximations that may be used in aircraft performance optimization.

Point-Mass Approximations

For aircraft capable only of subsonic speeds the quasi-steady approximation, where accelerations are neglected completely, is adequate for performance analysis.[1] However, the subsonic acceleration capability of supersonic aircraft is so great that it cannot be neglected if accurate performance prediction is desired. Furthermore the kinetic energy ($\frac{1}{2}mV^2$) of an aircraft flying at supersonic speeds is comparable to its gravitational potential energy (mgh), relative to the ground and thus, it is possible to trade velocity for altitude or vice versa. At subsonic speeds, the kinetic energy is almost negligible compared to the potential energy.

The latter considerations led to an improved approximation which we shall call the energy-state approximation§ where, indeed, it is assumed that kinetic and potential energy can be traded back and forth in zero time without loss of total energy.[2-5] Although performance optimization using this approximation often leads to unrealistic discontinuities in velocity and altitude, these correspond closely to zoom climbs or dives that appear in more accurate solutions. Total energy may be considered as the state variable of the system, and is continuous.

A further improvement in accuracy, at the sacrifice of added complexity, is to treat both velocity and altitude as state variables (they are then continuous) with flight-path angle as the control variable. Acceleration normal to the flight path is neglected and the resulting approximate equilibrium equation (lift = component of weight perpendicular to the flight path) is used to determine angle of attack.

The next most accurate approximation is to treat V, h, and γ as state variables with α as the control variable.[6,7] The mass may be approximated as a function of time. The most accurate approximation, short of considering out-of-plane motions or motions relative to the center of mass, is to treat V, h, γ, and m as state variables and α as the control variable.[8]

§ Also called the energy-climb approximation when applied to minimum time-to-climb or minimum fuel-to-climb problems.

Quasi-Steady Approximation

Both components of the acceleration are neglected leading to

$$0 \cong T(V,h) - D(\alpha,V,h) - mg\sin\gamma \tag{7}$$

$$0 \cong T(V,h)[\alpha + \epsilon] + L(\alpha,V,h) - mg\cos\gamma \tag{8}$$

where (7) and (8) express equilibrium parallel to and normal to the flight path, respectively. To maximize the rate of climb [Eq. (3)] at a given altitude, one may choose α to maximize $V\sin\gamma$ subject to the constraints (7) and (8), which determine V and γ for given values of h and α. Multiplying (7) by V/mg, we have

$$V\sin\gamma = V(T - D)/mg \tag{9}$$

Assuming $\cos\gamma \approx 1$, we may use (8) to determine $\alpha(V,h)$ and find V for a given h to maximize the excess power, the right-hand side of Eq. (9).

Energy-State Approximation

Here, the total energy per unit mass E is considered a state variable

$$E = \tfrac{1}{2}V^2 + gh \tag{10}$$

The time rate of change of E is obtained by differentiating (10) and using (1) and (3) to eliminate $\dot{V}$ and $\dot{h}$

$$\dot{E} = V(T - D)/m \tag{11}$$

Since the flight-path angle does not appear in (11), it is possible to use only the one state variable E for performance optimization if the acceleration normal to the flight path ($V\dot{\gamma}$) is neglected, and if nearly horizontal flight is assumed ($\cos\gamma \cong 1$). It is usually reasonable to neglect also the component of thrust normal to the flight path [$T\sin(\alpha + \epsilon)$]. With these approximations, Eq. (8) becomes simply

$$L(\alpha,V,h) \cong mg \tag{12}$$

which may be used to determine α in terms of V and h, i.e.,

$$\alpha = \alpha(V,h) \tag{13}$$

Furthermore, h may be expressed in terms of E and V

$$h = (E - \tfrac{1}{2}V^2)/g \tag{14}$$

Thus, V may be regarded as a control variable since both h and α can be expressed in terms of V and the state variable E.

Minimum Time to Climb

To minimize the time to climb to a given altitude and velocity using the energy-state approximation, it is clear that we must maximize $\dot{E}$ with respect to V for a given E, i.e.,

$$\max_V \{V[T(E,V) - D(E,V)]\} \tag{15}$$

Table 1 Lift and drag coefficients as a function of angle of attack and Mach number for airplane 1

M	0	0.4	0.8	0.9	1.0	1.2	1.4	1.6	1.8
$C_{L\alpha}$	3.44	3.44	3.44	3.58	4.44	3.44	3.01	2.86	2.44
C_{D_0}	0.013	0.013	0.013	0.014	0.031	0.041	0.039	0.036	0.035
η	0.54	0.54	0.54	0.75	0.79	0.78	0.89	0.93	0.93

$C_L = C_{L\alpha}\alpha$ $\quad L = C_L\frac{1}{2}\rho V^2 S$ $\quad S = 530$ ft^2

$C_D = C_{D_0} + \eta C_{L\alpha}\alpha^2$ $\quad D = C_D\frac{1}{2}\rho V^2 S$

Table 2 Lift and drag coefficients as a function of angle of attack and Mach number for airplane 2

M	0	0.4	0.8	1.2	1.6	2.0	2.4	2.8	3.2
C_{L_α}	2.240	2.325	2.350	2.290	2.160	1.950	1.700	1.435	1.250
C_{D_0}	0.0065	0.0055	0.0060	0.0118	0.0110	0.0086	0.0074	0.0069	0.0068
	$C_L = C_{L_\alpha}\alpha$				$L = C_L \frac{1}{2}\rho V^2 S$			$S = 500$ ft^2	
	$C_D = C_{D_0} + \eta C_{L_\alpha}\alpha^2$				$D = C_D \frac{1}{2}\rho V^2 S$			$\eta = 1.0$	

where h and α are expressed in terms of E and V.¶ This operation, in principle, allows us to express $V = V(E)$, a feedback law. Figure 2 shows a typical (h,V) plane with contours of constant E on it. A typical optimum flight path is sketched as the arcs BC and DF. It is possible to move along E = constant contours in zero time according to this approximation, so the minimum-time path from point A′ to G is a rapid dive to B′, motion along B′C to C, then a rapid dive from C to D, motion along DF to F, and a rapid climb (a zoom) to G.** Notice, however, that the rapid dive and climb portions may violate the assumption that $\cos\gamma \cong 1$. If the initial zoom dive from point A′ goes below $h = 0$, obviously the constraint $h \geq 0$ requires leveling out and flying just above $h = 0$ to point B; takeoff is such a special case where the initial altitude is zero (for example, point A).

Data on lift, drag, thrust, and fuel consumption are given in Tables 1–4 for two different supersonic airplanes. Airplane 1 is the same one considered in Ref. 8, whereas airplane 2 is the same as the one used in Ref. 9.

Contours of constant excess power are shown in Figs. 3 and 4 for airplanes 1 and 2, respectively, along with contours of constant energy-height E/g. The minimum time-to-climb paths are also shown, being the loci of points yielding the maximum excess power at a fixed energy. Note that the path for airplane 1 exhibits a discontinuity in velocity (a zoom dive) near Mach number 1, whereas the path for airplane 2 does not.

The minimum time-to-climb path for airplane 1 to get to $M = 1.0$ and $h = 65{,}600$ ft (20 km) is shown in Fig. 5. It consists of an accelerating flight at sea level from $M = 0.38$ to $M = 0.87$, a climb at nearly constant Mach number ($M \cong 0.93$) to $h = 35{,}000$ ft, a rapid dive to 24,000 ft and $M = 1.25$, an increasing Mach number climb to $h = 35{,}000$ ft and $M = 1.75$, and finally, a zoom climb to $h = 65{,}600$ ft and $M = 1.0$. The minimum-time path computed with four state variables using steepest descent[8] is also shown. By rounding off corners, the energy-climb path is reasonably close to the more accurate path. However, the time estimate on the energy-climb path (from $h = 0$, $M = 0.38$) is 277 sec plus time to dive and to zoom; using the times from the four state variable solution for these segments (40 sec for dive, 60 sec for zoom climb) gives 377 sec. The time for the four state variable solution with an initial weight of 42,000 lb is 332 sec.

Table 3 Thrust and fuel consumption[a] as a function of altitude and Mach number for airplane 1

	Thrust T (thousands of lb)									
Mach no. M	Altitude h (thousands of ft) 0	5	10	15	20	25	30	40	50	70
0	24.2									
0.2	28.0	24.6	21.1	18.1	15.2	12.8	10.7			
0.4	28.3	25.2	21.9	18.7	15.9	13.4	11.2	7.3	4.4	
0.6	30.8	27.2	23.8	20.5	17.3	14.7	12.3	8.1	4.9	
0.8	34.5	30.3	26.6	23.2	19.8	16.8	14.1	9.4	5.6	1.1
1.0	37.9	34.3	30.4	26.8	23.3	19.8	16.8	11.2	6.8	1.4
1.2	36.1	38.0	34.9	31.3	27.3	23.6	20.1	13.4	8.3	1.7
1.4		36.6	38.5	36.1	31.6	28.1	24.2	16.2	10.0	2.2
1.6				38.7	35.7	32.0	28.1	19.3	11.9	2.9
1.8						34.6	31.1	21.7	13.3	3.1

[a] $f = T/cg$ slugs/sec, where $c = 1600$ sec.

¶ Note the only difference between this and the quasi-steady approximation is holding E = const instead of h = const in maximizing $V(T - D)$.

** Arcs CD and FG are corners, i.e., places where the control variable V is discontinuous.

Minimum Fuel to Climb

To minimize fuel to climb to a given altitude and velocity using the energy-state approximation, we use the expression for fuel consumption at maximum throttle (5) and divide it into (11) to obtain

$$-dm/m = f(E,V)dE/V[T(E,V) - D(E,V)] \quad (16)$$

Clearly we must maximize $V(T - D)/(-\dot{m})$ to minimize the fuel consumed in arriving at a certain energy level.

Contours of constant energy increase per lb of fuel burned, $V(T - D)/(-\dot{m}g)$, are shown in Figs. 6 and 7 for airplanes 1 and 2, respectively. The minimum fuel-to-climb paths are also shown, being the loci of maximum energy increase per lb of fuel burned at fixed energy E. The minimum fuel-to-climb path for airplane 1 to get to $h = 65{,}600$ ft and $M = 1.0$, is qualitatively similar to the minimum-time path. However, it does go higher during the subsonic climb to $h = 44{,}000$ ft and dives only to $h = 33{,}000$ ft at $M = 1.30$. Similarly, the minimum fuel-to-climb path for airplane 2 is generally similar to but consistently above the minimum-time path. No four state variable solution was available for the minimum-fuel climb when this paper was written.

Minimum-Range Glide

Within the energy-state approximation $\cos\gamma \cong 1$, the horizontal range rate [Eq. (4)] is given by

$$\dot{x} = V \quad (17)$$

Dividing (17) into (11) and considering the case $T = 0$ (gliding flight), gives

$$dE/dx = -D(E,V)/m \quad (18)$$

Clearly, to maximize range we should minimize the magnitude

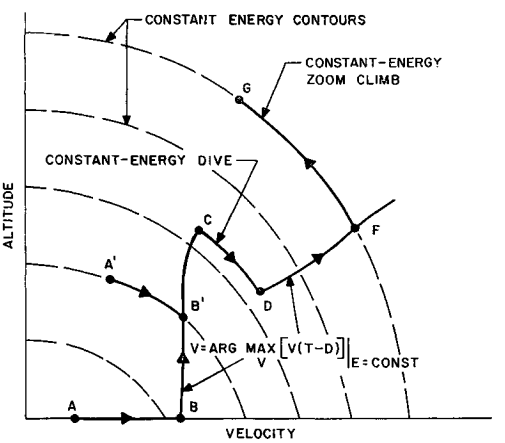

Fig. 2 Sketch of a typical minimum-time energy-climb path.

Table 4 Thrust and fuel consumption[a] as a function of altitude and Mach number for airplane 2

Mach no. M	Thrust T (thousands of lb) Altitude h (thousands of ft) 0	5	15	25	35	45	55	65	75	85	95	105
0	23.3	20.6	15.4	9.9	5.8	2.9	1.3	0.7	0.3	0.1	0.1	0.0
0.4	22.8	19.8	14.4	9.9	6.2	3.4	1.7	1.0	0.5	0.3	0.1	0.1
0.8	24.5	22.0	16.5	12.0	7.9	4.9	2.8	1.6	0.9	0.5	0.3	0.2
1.2	29.4	27.3	21.0	15.8	11.4	7.2	3.8	2.7	1.6	0.9	0.6	0.4
1.6	29.7	29.0	27.5	21.8	15.7	10.5	6.5	3.8	2.3	1.4	0.8	0.5
2.0	29.9	29.4	28.4	26.6	21.2	14.0	8.7	5.1	3.3	1.9	1.0	0.5
2.4	29.9	29.2	28.4	27.1	25.6	17.2	10.7	6.5	4.1	2.3	1.2	0.5
2.8	29.8	29.1	28.2	26.8	25.6	20.0	12.2	7.6	4.7	2.8	1.4	0.5
3.2	29.7	28.9	27.5	26.1	24.9	20.3	13.0	8.0	4.9	2.8	1.4	0.5

[a] $f = T/cg$ slugs/sec, where $c = 2800$ sec.

of dE/dx, i.e.,

$$\min_V D(E,V) \text{ for fixed } E \tag{19}$$

subject to the constraint that $L = mg$ [Eq. (12)], and using (14) to express h in terms of E and V. For airplanes 1 and 2, this minimum is indistinguishable from the minimum with respect to V holding altitude h constant.

If the initial conditions are not on the maximum range glide path, the airplane should either zoom climb or zoom dive, with constant energy, to the maximum range curve (see Fig. 8). At $h = 0$, no minimization is possible, and to stay airborne one must accept the drag associated with $L = mg$, losing speed (and increasing α) until stalling speed is reached.

The range covered is given by (18) as

$$R = \int_{E_1}^{E_0} \frac{mdE}{D_{\min}(E)} + \int_{E_s}^{E_1} \frac{mVdV}{[D(V)]_{h=0}} \tag{20}$$

where E_0 = initial energy, E_1 = energy at $h = 0$ at minimum drag for $L = mg$, and E_s = energy at $h = 0$ at stalling speed and $L = mg$. If the initial velocity is supersonic, the range given by (20) is considerably greater than the range estimated using the quasi-steady approximation, namely

$$R = \int_0^{h_0} \frac{mg}{D_{\min}(h)} dh = \left(\frac{\bar{L}}{D}\right)_{\max} h_0 \tag{21}$$

where $(\overline{L/D})_{\max}$ is the average value of $(L/D)_{\max}$ along the path. This is explained by the fact that initially the vehicle dissipates its kinetic energy against drag while maintaining almost constant potential energy (i.e., altitude), and only toward the end of the glide does the vehicle dissipate its potential energy. The quasi-steady approximation considers only the dissipation of the vehicle's potential energy. Another way to view this phenomenon is to use Eq. (1) to express $\dot{h} = V \sin\gamma$ for $T = 0$:

$$\dot{h} = V \sin\gamma = -V[(D/mg) + (\dot{V}/g)] \tag{22}$$

Dividing Eq. (22) by Eq. (17), we have the slope of the glide path:

$$(dh/dx) \cong -(D/mg) - (\dot{V}/g) \tag{23}$$

Since $\dot{V} < 0$ along the glide path, the second term on the right-hand side of Eq. (23) appears to decrease the drag and thus stretch the glide.

Using the aerodynamic data of Tables 1 or 2, we have

$$D/mg = (C_{D_0}qS/mg) + [\eta(mg)/C_{L_\alpha}qS] \tag{24}$$

where $q = \frac{1}{2}V^2\rho(h)$. Figure 9 shows contours of constant drag for lift = weight and the Mach number-altitude profile of the maximum range glide path for airplane 2 at a weight of 34,200 lb.

Maximum Range at a Fixed Throttle for a Given Amount of Fuel

To obtain maximum range for a given amount of fuel at a fixed throttle setting, using the energy state approximation, it is convenient to let the fuel mass used be the independent variable instead of time or range. Let

$$\mu = m_0 - m = \text{fuel mass used} \tag{25}$$

Dividing (5) into (11) and using (25), we have

$$dE/d\mu = V(T - D)/f(m_0 - \mu); \quad E(O) \text{ specified} \tag{26}$$

As in the climb problems, it is also necessary to consider the

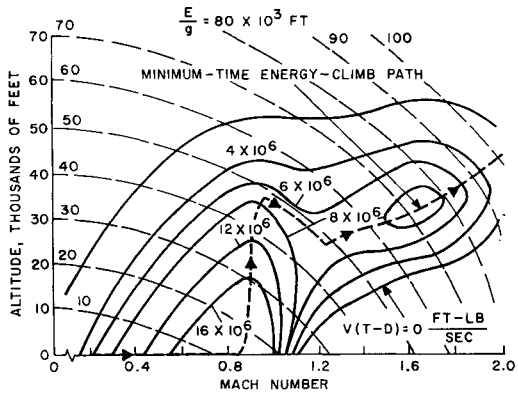

Fig. 3 Contours of constant excess power and minimum-time energy-climb path (airplane 1).

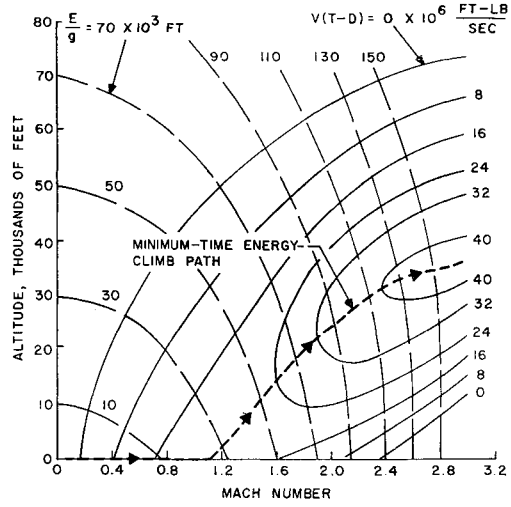

Fig. 4 Contours of constant excess power and minimum-time energy-climb path (airplane 2).

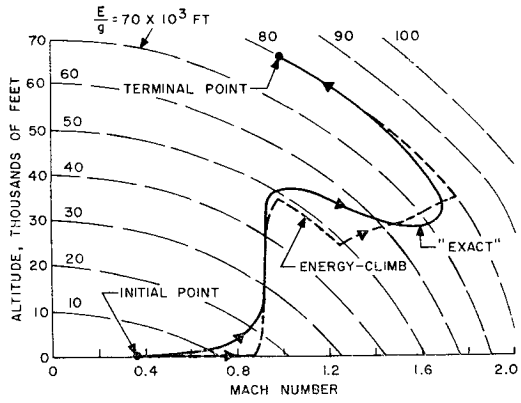

Fig. 5 Comparison of exact and energy-state minimum time-to-climb paths (airplane 1).

constraint

$$V_s \leq V \leq (2E)^{1/2} \tag{27}$$

where $V_s(E)$ is the stalling speed and $V \leq (2E)^{1/2}$ insures $h \geq 0$.

The range may be written in terms of μ through use of Eq,. (5), (17), and (25):

$$R = \int_0^{\mu_f} \frac{V d\mu}{f(E,V)} \tag{28}$$

where μ_f = amount of fuel to be used in the flight.

Now (28) can not be maximized by simply maximizing V/f with respect to V for fixed E. This maximum turns out to be at $h > 0$ for all E, and there is no way of getting to this altitude with $V > V_s$ from takeoff without first putting some energy into the vehicle. Thus, we expect that the optimum path will start out very close to the path that maximizes the right-hand side of Eq. (26); this is the same path used for minimum fuel to climb. However, after gaining some energy, the path will move up to high altitudes where the integrand of Eq. (28) is large.

Using the calculus of variations, the optimal path can be found by solving a fairly simple two-point boundary value problem. The variational Hamiltonian is

$$H = (V/f) + \lambda[V(T - D)/f(m_0 - \mu)] \tag{29}$$

The influence function λ must therefore satisfy

$$d\lambda/d\mu = -\partial H/\partial E|_V \tag{30}$$

and, since final energy is not specified,

$$\lambda(\mu_f) = 0 \tag{31}$$

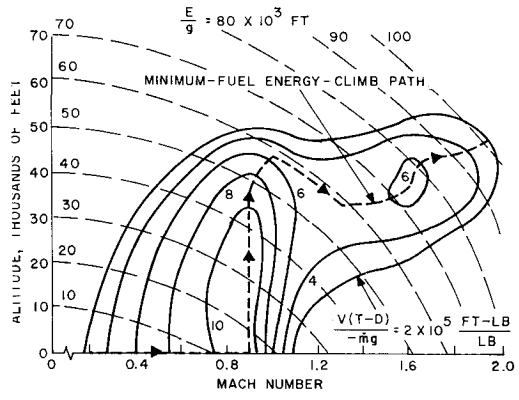

Fig. 6 Contours of constant energy increase per lb of fuel burned and minimum-fuel energy-climb path (airplane 1).

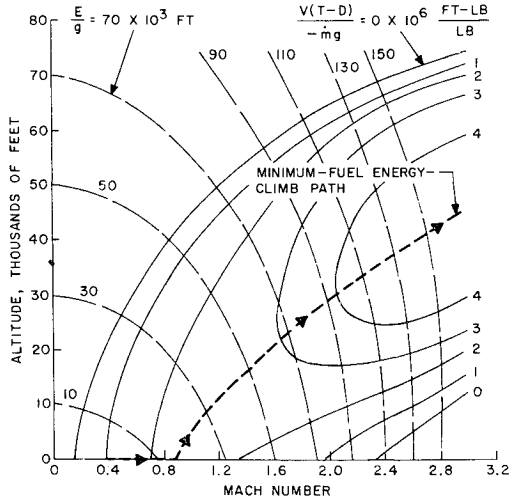

Fig. 7 Contours of constant energy increase per lb of fuel burned and minimum-fuel energy-climb path (airplane 2).

The optimality condition is

$$V = \arg\max_V H(V,E,\mu,\lambda) \tag{32}$$

except on the constraints (27) where $V = (2E)^{1/2}$ or $V = V_s(E)$. The two-point boundary value problem consists of solving Eqs. (26), (30), (31), and (32), simultaneously, keeping in mind (27).

At takeoff, λ is large, so from (29) and (32), the flight path is close to the minimum fuel-to-climb curve [maximum of $V(T - D)/f$ with respect to V for given E]. Near the end of powered flight, λ is small, and the flight path is close to maximum altitude where the largest values of V/f occur.

Figure 10 shows the Mach number-altitude path for maximum range at full throttle for airplane 2 using 2400 lb of fuel with a takeoff weight of 36,000 lbs. Note that it starts off on $h = 0$, then climbs very close to the curve for maximum $V(T - D)/f$, and veers up sharply to high altitude near the end of the flight. The terminal point of a four state variable solution to the same problem[9] is also shown in Fig. 10. Note that the present solution achieves about 7% more range, which may be due to the fact that, in Ref. 9, a quasi-steady constant-altitude cruise condition was assumed for the final segment of the flight.

Maximum Range for a Given Amount of Fuel Using Full Throttle Followed by a Glide

To obtain the maximum total range for a given amount of fuel, clearly the powered part of the flight ($T \neq 0$) will be

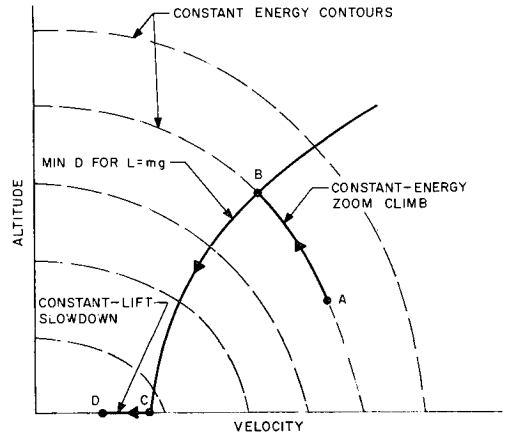

Fig. 8 Sketch of a typical maximum-range glide path.

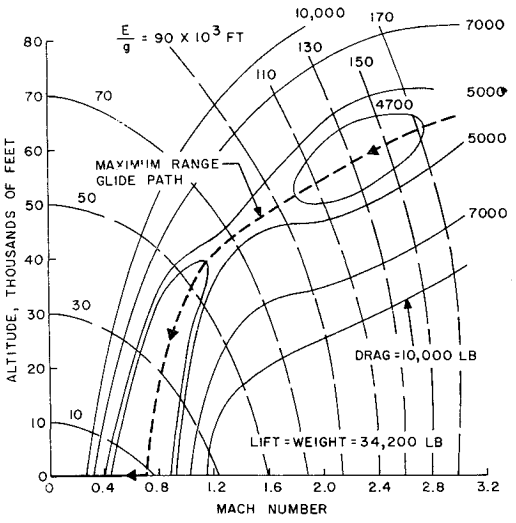

Fig. 9 Contours of constant drag for lift = weight and maximum-range glide path (airplane 2).

followed by a maximum-range glide. Thus, the range may be written as

$$R = \phi(E_f) + \int_0^{t_f} V dt \tag{33}$$

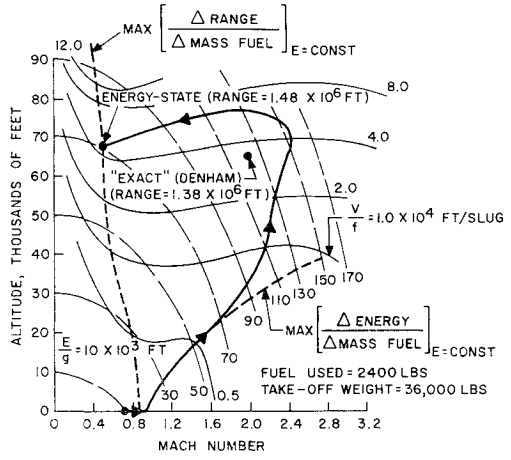

Fig. 10 Maximum-range path at full throttle for a given amount of fuel (airplane 2).

where $\phi(E_f)$ = maximum range for an unpowered glide starting at energy E_f and t_f is the time when powered flight ends.

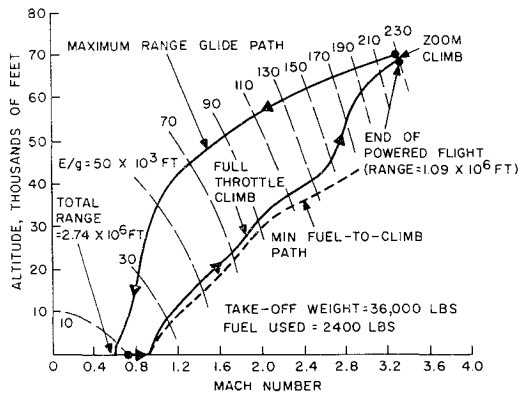

Fig. 11 Maximum total range path for a given amount of fuel (airplane 2).

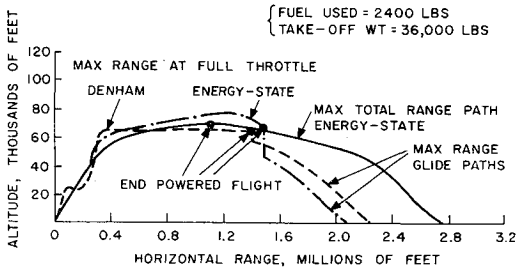

Fig. 12 Maximum-range profiles for a given amount of fuel (airplane 2).

It is again convenient to use $m_0 - m = \mu$ (fuel mass used) as the independent variable instead of time. It seems likely that for long flights, the powered part of the flight will contain a cruise portion that uses less than maximum thrust (partial throttle). However, data on fuel consumption at partial throttle were not available to the authors. Therefore, as a first step in exploring the use of the energy-state approximation for maximum-range problems, full thrust was used for the powered part of the flight. Using (28) we have

$$R = \phi(E_f) + \int_0^{\mu_f} \frac{V d\mu}{f(E,V)} \tag{34}$$

The two-point boundary value problem to be solved is almost the same as the previous one [Eqs. (26), (27), (30) and (32)]. The only difference is that Eq. (31) is replaced by

$$\lambda(\mu_f) = \partial\phi/\partial E_f \tag{35}$$

An expression for the boundary condition (35) can be obtained from (18):

$$\lambda(\mu_f) = m_f/D_{\min}(E_f) \tag{36}$$

which turns out to be relatively insensitive to the final energy E_f.

Figure 11 shows the Mach number-altitude path for maximum total range for airplane 2 using 2400 lb of fuel with a takeoff weight of 36,000 lb. This path starts out very much like the path of Fig. 10, but instead of going to a very high altitude near the end of powered flight, it goes to a very high energy level to take advantage of the long supersonic glide. At the end of powered flight, there is a short constant-energy zoom climb to the maximum-range glide path (which is the same as the one shown in Fig. 9).

Figure 12 shows the range vs altitude profiles for the maximum-range paths that correspond to Figs. 10 and 11. Maximum-range glide curves have been added to the paths shown in Fig. 10 to clearly illustrate that they are not maximum total range paths.

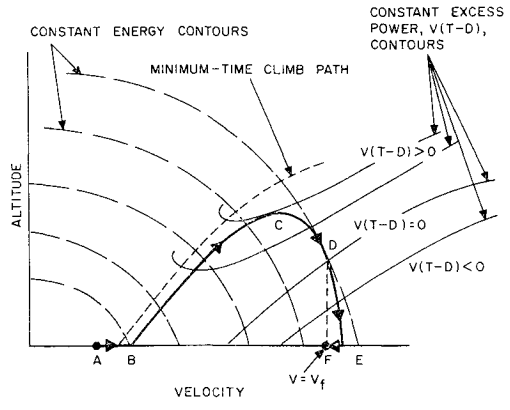

Fig. 13 Sketch of a typical path for maximum range in a given time.

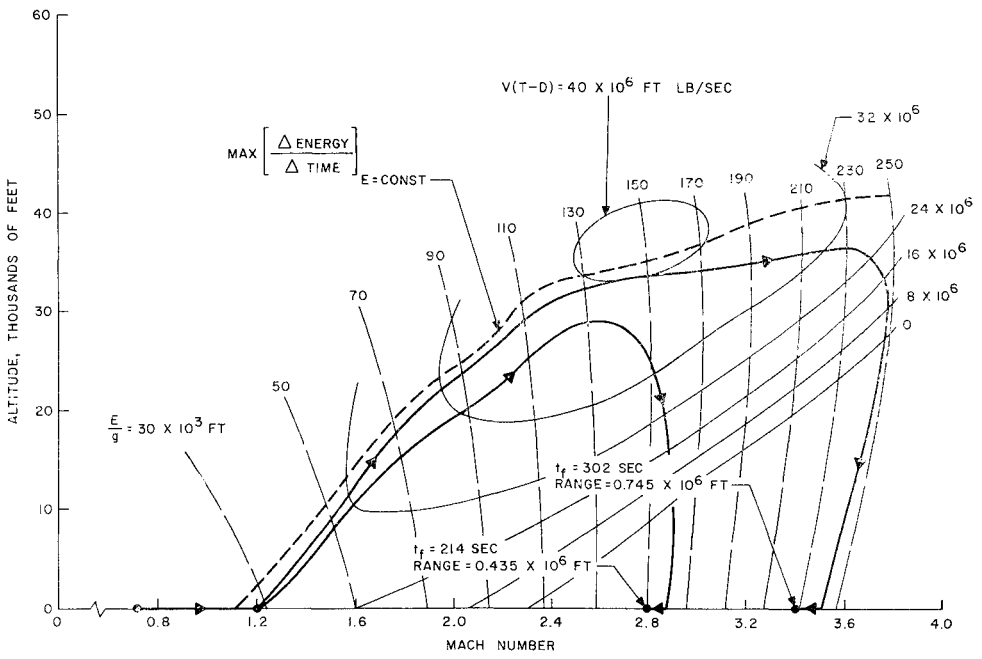

Fig. 14 Maximum - range paths for a given time (airplane 2).

Maximum Range in a Given Time

From Eq. (17), the range covered in a given time interval, $0 \leq t \leq t_f$ is

$$R = \int_0^{t_f} V dt \tag{37}$$

To determine the flight profile for maximum range, the integral in (37) must be maximized subject to Eqs. (11), (27), and (5), with initial energy specified. If we neglect the mass variation and use an average mass in Eq. (11), then Eq. (5) is not needed and the problem has only one state variable E. (A more accurate estimate would be obtained by using an estimate of m as a function of time.) This is a calculus of variations problem in which the constraint $V \leq (2E)^{1/2}$ (i.e., $h \geq 0$) plays an important role. The variational Hamiltonian is

$$H = V + \lambda[V(T - D)/m] \tag{38}$$

where the influence function λ must satisfy

$$\lambda(t_f) = 0 \tag{39}$$

since the final energy is not specified.

It is not necessary to solve the Euler-Lagrange differential equation for λ in this case because H = const is an integral of the two-point boundary value problem. In fact, applying (39) to (38), we see that

$$H = V(t_f) \triangleq V_f \tag{40}$$

Using (40) in (38), we may solve for $\lambda(t)$:

$$\lambda(t) = (V_f - V)/V(T - D)m \tag{41}$$

The optimality condition is

$$V = \arg \max_V H(E,V,\lambda) \tag{42}$$

where $V \leq (2E)^{1/2}$. Note the maximum operation is performed in (42) with E and λ fixed. If the maximum occurs for $V < (2E)^{1/2}$, then

$$\partial H/\partial V|_E = 0 \text{ or } 0 = 1 + (\lambda/m)(\partial/\partial V)[V(T - D)] \tag{43}$$

Substituting (41) into (43) yields the optimality condition

$$(\partial/\partial V)[V(T - D)] = -V(T - D)/V_f - V \quad \text{if } V < (2E)^{1/2} \tag{44}$$

The value of V_f depends, of course, on t_f and must be determined by iteration.

Examining (38) in view of (42), it is clear that the optimal path will start (with λ large) near, but at an altitude below, the path of maximum excess power, $V(T - D)$. As the flight progresses (with decrease in λ), the optimal path will veer toward $h = 0$ where V is large. The optimal path will spend some time near (and including) the end of the flight on the constraint boundary $h = 0$, i.e., $V = (2E)^{1/2}$. Figure 13 shows a sketch of the velocity-altitude path for maximum range in a given time. Segment AB is on $h = 0$. Arc BCD is an increasing energy path with the initial part of the arc just below the minimum-time climb path. At point D where excess power $V(T - D)$ is zero, the airplane has maximum energy with $V = V_f$. Arc DE is a powered flight with decreasing energy $(T - D < 0)$ and segment EF is a dash just above the ground at $h = 0$. It can be shown from (44) that the time taken in the descent portion of the optimal path depends on the curvature of $V(T - D)$ with respect to V, at a fixed value of E, the descent being more rapid at lesser values of curvature. The possibility of a short constant-energy zoom dive (in general, not all the way to $h = 0$) arises in cases when either $V(T - D)$ has two local maxima with respect to V at a fixed value of E or $V(T - D)$ varies linearly with respect to V at a fixed value of E, the zoom dive being over the range of linear variation in the latter case. A zoom dive all the way to $h = 0$ occurs if the curvature of $V(T - D)$ with respect to V is nonnegative at $h = 0$ at a fixed value of E.

Figure 14 shows two Mach number vs altitude paths for maximum range for given times $t_f = 214$ sec and $t_f = 302$ sec, respectively. The optimal path for $t_f = 302$ sec starts out closer to the minimum-time climb path, attaining higher energy in the process, before it veers to the ground towards the end of flight to take advantage of the larger values of V. Note that the constant energy curves are not parabolas in the altitude vs Mach number space. The final part of this flight path undoubtedly exceeds dynamic pressure limitations and engine constraints. If these in-flight constraints were known, an optimal path could be found that satisfies them.

Conclusions

The energy-state approximation, properly interpreted, is quite adequate for performance optimization of super-

sonic aircraft. In addition to its use for determining flight profiles for minimum time to climb to a given altitude and speed, and minimum fuel to climb to a given altitude and speed, this paper shows that the energy-state approximation may also be used to determine flight profiles for 1) maximum-range glide from a given altitude and speed to another altitude and speed; 2) maximum range at a fixed throttle setting for a given amount of fuel (or, what is the equivalent problem, minimum fuel for a given range at a fixed throttle setting); 3) maximum total range for a given amount of fuel (or minimum fuel for a given total range); 4) maximum range in a given time (or minimum time for a given range).

References

[1] Perkins, C. D. and Hage, R. E., *Airplane Performance, Stability, and Control*, Wiley, New York, 1949, pp. 175–182.

[2] Lush, K. J., "A Review of the Problem of Choosing a Climb Technique with Proposals for a New Climb Technique for High Performance Aircraft," R and M 2557, 1951, British Aeronautical Research Council.

[3] Rutowski, E. S., "Energy Approach to the General Aircraft Performance Problem," *Journal of Aeronautical Science*, Vol. 21, No. 3, March 1954, pp. 187–195.

[4] Lush, K. J. et al., "Total Energy Methods," *AGARD Flight Test Manual*, Vol. 1, 1954, Chap. 7.

[5] Kelley, H. J., "An Investigation by Variational Methods of Flight Paths for Optimum Performance," Ph.D. thesis, New York Univ., May 1958.

[6] Miele, A., "Minimal Maneuvers of High Performance Aircraft in a Vertical Plane," TN D-155, Sept. 1959, NASA.

[7] Miele, A., *Flight Mechanics I—Theory of Flight Paths*, Addison-Wesley, Reading, Mass., 1962.

[8] Bryson, A. E. and Denham, W. F., "A Steepest-Ascent Method for Solving Optimum Programming Problems," *Journal of Applied Mechanics*, Vol. 29, June 1962.

[9] Denham, W. F., "Steepest-Ascent Solution of Optimal Programming Problems," Ph.D. dissertation, Div. of Engineering and Applied Physics, Harvard Univ., 1963, Chap. 6.

NOV.-DEC. 1969 J. AIRCRAFT VOL. 6, NO. 6

Lifting-Surface Theory for V/STOL Aircraft in Transition and Cruise. I

E. S. LEVINSKY*, H. U. THOMMEN†, P. M. YAGER‡, AND C. H. HOLLAND‡
Air Vehicle Corporation, San Diego, Calif.

This is the first part of a two-part paper in which a large-tilt-angle lifting-surface theory is developed for tilt-wing and tilt-propeller (or rotor) type V/STOL aircraft. Part I deals with the development of an inclined actuator disk analysis which forms the basis of the method. Closed form solutions are obtained for the velocity potential at large distances behind the actuator surface. Both the normal velocity and the nonlinear pressure boundary conditions are satisfied across the slipstream interface. Effects of slipstream rotation are also evaluated. In Part II, the included actuator disk analysis is combined with a discrete-vortex Weissinger-type lifting-surface theory for application to wing-propeller combinations at arbitrary tilt angle and forward speed.

Nomenclature

A_p = propeller area
A_s = area of fully contracted propeller slipstream
b = wing span
C_{D_0} = zero lift drag coefficient
C''_{H_p} = propeller horizontal force coefficient based on propeller area and slipstream total pressure
C''_{L_p} = propeller vertical force coefficient based on propeller area and slipstream total pressure
C_l = section lift coefficient based on q_∞
C_{l_a} = section ideal lift coefficient
C, D = unknown coefficients in Eqs. (4) and (5)
C''_n = section normal force coefficient based on slipstream total pressure
c = wing chord length
$\mathbf{D}$ = drag force
$\mathbf{e}_r, \mathbf{e}_x, \mathbf{e}_\theta$ = unit vectors in cylindrical coordinate system
$\mathbf{e}_z$ = unit vector in z direction
F = complex potential (inclined actuator disk theory)
G = integral defined by Eq. (24)
$g(\mu)$ = function of $\mu = (1 + \mu)(1 - \mu)^{-1}G_o$
H = total pressure
h = one-half of the vortex spacing on the wing
I = integral defined by Eq. (24), also number of wing control stations
i = $(-1)^{1/2}$
J = propeller advance ratio
K = number of slipstreams
L = lift force
M = number of slipstream control points
N = propeller revolutions/sec
n = normal force/unit span
P, P' = power, also potential influence function (P' for multiple slipstreams)
p = static pressure
q = dynamic pressure
R = radius of fully contracted slipstream
R_c = radius of cylindrical control surface
R_p = propeller radius
r, θ = cylindrical coordinates, slipstream coordinate system
S = surface area, also downwash velocity influence coefficient
T = propeller thrust
T''_c = propeller thrust coefficient = $T/A_p(q_\infty + \Delta H)$
u, v, w = velocity components in slipstream coordinate system
V = velocity
V_γ = induced velocity inside slipstream

Received September 26, 1968; revision received April 23, 1969. The research was supported by the U. S. Army Aviation Material Laboratories under Contract No. DAAJ02-67-C-0059, and has been reported in more detail in Ref. 15.

* Vice President. Member AIAA.

† Former Staff Scientist, now Professor at Southeastern Massachusetts Technical Institute, Department of Mechanical Engineering, North Dartmouth, Mass.

‡ Staff Scientists.